Materials Letters 139 (2015) 104–107

Contents lists available at ScienceDirect

Materials Letters

journal homepage: www.elsevier.com/locate/matlet

Characterization of multiferroic $Bi_{0.8}RE_{0.2}FeO_3$ powders (RE = Nd^{3+}, Eu^{3+}) grown by the sol–gel method

A.H. Reshak [a,b,*], T. Slimani Tlemçani [c], T. El Bahraoui [c], M. Taibi [d], K.J. Plucinski [e], A. Belayachi [c], M. Abd-Lefdil [c], M. Lis [f], Z.A. Alahmed [g], H. Kamarudin [b], J. Chyský [h], J. Bila [h]

[a] New Technologies – Research Center, University of West Bohemia, Univerzitni 8, 306 14 Pilsen, Czech Republic
[b] Center of Excellence Geopolymer and Green Technology, School of Material Engineering, University Malaysia Perlis, 01007 Kangar, Perlis, Malaysia
[c] University of Mohammed V, Materials Physics Laboratory, P.B. 1014, RABAT, MOROCCO
[d] University of Mohammed V- Agdal, Laboratoire de Physico-Chimie des Matériaux Inorganiques et Organiques, Ecole Normale Supérieure Rabat-Morocco
[e] Electronics Department, Military University Technology, Kaliskiego 2, Warsaw 00-908, Poland
[f] Electrical engineering Department, Czestochowa University Czestochowa, Armii Krajowej 17, Czestochowa, Poland
[g] Department of Physics and Astronomy, King Saud University, Riyadh 11451, Saudi Arabia
[h] Department of Instrumentation and Control Engineering, Faculty of Mechanical Engineering, CTU in Prague, Technicka 4, 166 07 Prague 6, Czech Republic

ARTICLE INFO

Article history:
Received 31 August 2014
Accepted 6 October 2014
Available online 23 October 2014

Keywords:
Sol–gel method
Powders
Photoinduced

ABSTRACT

A possibility of changes the non-linear optical response was shown for the first time in the $BiFeO_3$ doped by the Eu and Nd materials synthesized by the sol–gel method. Grain size here plays a substantial role. At the same time the latter is responsible for the non-linear optical response. The photoinduced optics was performed by the Nd:YAG lasers of different powers for samples of different nanosizes.

1. Introduction

Rare-earth substituted multiferroic $BiFeO_3$ (BFO) powders with chemical compositions of $Bi_{0.8}RE_{0.2}FeO_3$ (RE = Nd^{3+}, Eu^{3+}) were synthesized by the sol–gel method. The RE^{3+} substituted BFO (RE-BFO) materials lead to change of the $BiFeO_3$ crystal structure from rhombohedral to pseudocubic symmetry. Thermal and transmission electron microscopy (TEM) investigation of the synthesized compounds confirms that the substitution has an important effect on the physical properties and on the grain size of the particles [1–6].

The treatment was performed similarly to that described in Refs. [7–12]. The main goal of the research is the possible exploration of the titled material for the optically operated triggers.

2. Experiment

Powders of $Bi_{0.8}RE_{0.2}FeO_3$ (RE = Nd^{3+}, Eu^{3+}) were synthesized by the sol–gel method. $Bi(NO_3)_3.5H_2O$, $Fe(NO_3)_3.9H_2O$, $Nd(NO_3)_3.6H_2O$ and $Eu(NO_3)_3.6H_2O$ were used as starting materials. They were separately dissolved into glacial acetic acid. Ethylene glycol was added under constant stirring. After stirring for one hour, bismuth solution and iron solution were mixed together. The mixture was stirred at 40 °C and the resulting gel samples were dried at 60 °C for about 20 hours to obtain BFO dried gel. The dried gel was ground in an agate mortar. Finally the samples were annealed at 500 °C in air for 12 hours.

The crystal symmetry was determined by X-ray diffraction (XRD) measurements. Transmission electron microscopy (TEM) was used to observe the powder surface morphology and estimate the particle size. The Neel temperature (T_N) of the samples was measured by differential scanning calorimetry (DSC). Differential thermal analysis (DTA) was used to determine the ferroelectric phase transition temperature (T_C).

3. Results and discussion

The XRD patterns of $BiFeO_3$ (BFO) and rare earth substituted BFO powders $Bi_{0.8}Nd_{0.2}FeO_3$ (Nd-BFO) and $Bi_{0.8}Eu_{0.2}FeO_3$ (Eu-BFO) (Fig. 1a) show the presence of a single phase. The results indicate that the BFO compound crystallizes in the typical rhombohedral lattice with space group R3c (α-phase) with $a = 0.5625 \pm 0.0005$ nm and $c = 1.3575 \pm 0.0012$ nm. RE doped $BiFeO_3$ shows gradual variation in

* Corresponding author at: New Technologies - Research Center, University of West Bohemia, Univerzitni 8, 306 14 Pilsen, Czech Republic.
E-mail address: maalidph@yahoo.co.uk (A.H. Reshak).

http://dx.doi.org/10.1016/j.matlet.2014.10.034
0167-577X/

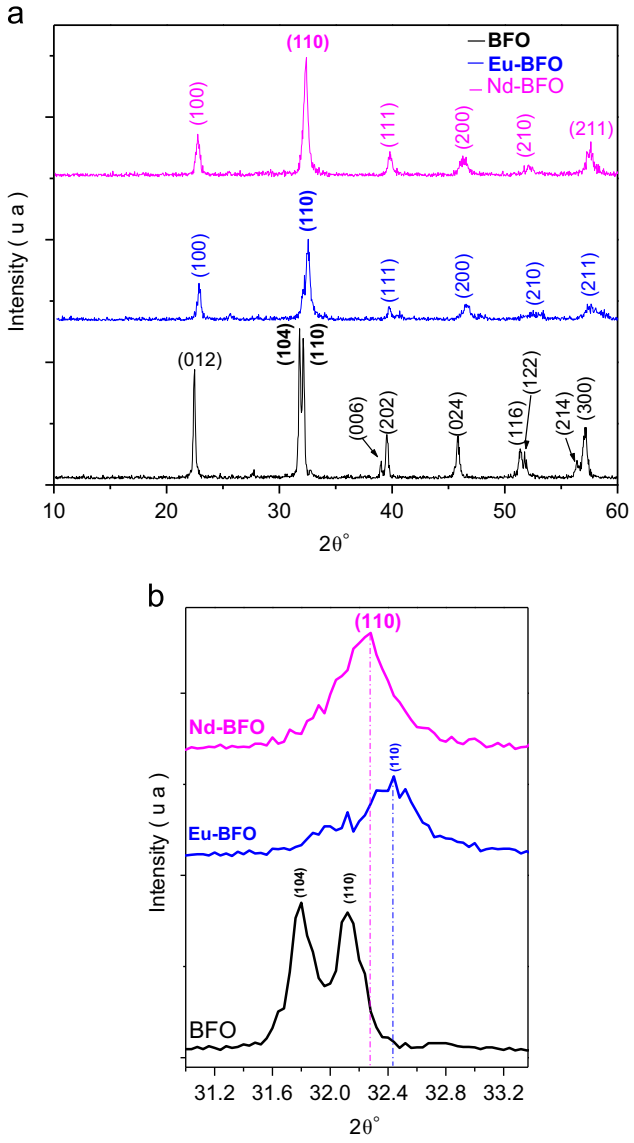

Fig. 1. (a) XRD patterns of BFO, Nd-BFO and Eu-BFO powders. (b) Magnified patterns in the vicinity of $2\theta = 32^\circ$.

peaks when compared with parent $BiFeO_3$, the combination of neighboring peaks in the 2θ degrees of 31°–33°, 38.5°–40°, 51°–52° and 56°–57°. Fig. 1b represents a magnified pattern around $2\theta =$ 31°–33°. We can note that the lines (1 0 4) and (1 1 0) are clearly not split but overlapped completely and combine into a single line (1 1 0) in the X-ray diffractograms of RE-BFO samples. The above phenomenon confirms that the crystal symmetry was changed from the rhombohedral to pseudocubic one with space group Pm3m (γ-phase). The same behavior, the transition ($\alpha \rightarrow \gamma$), was observed in similar compounds [1,2].

The TEM investigation of the synthesized compounds is shown in Fig. 2. The pictures confirm that the matrixes are homogenate and no segregation of impurities is detected. In BFO samples the grains are found to be approximately spherical with an average grain size of around 60 nm. However, in the case of RE-BFO samples, the grains are found to be spherical with reduced grain size, 22 nm and 15 nm for Nd-BFO and Eu-BFO, respectively. Then, we can conclude that the substitution of bismuth by rare earth in the multiferroic material BFO is accompanied by a significant decrease of the grain size of the particles [3].

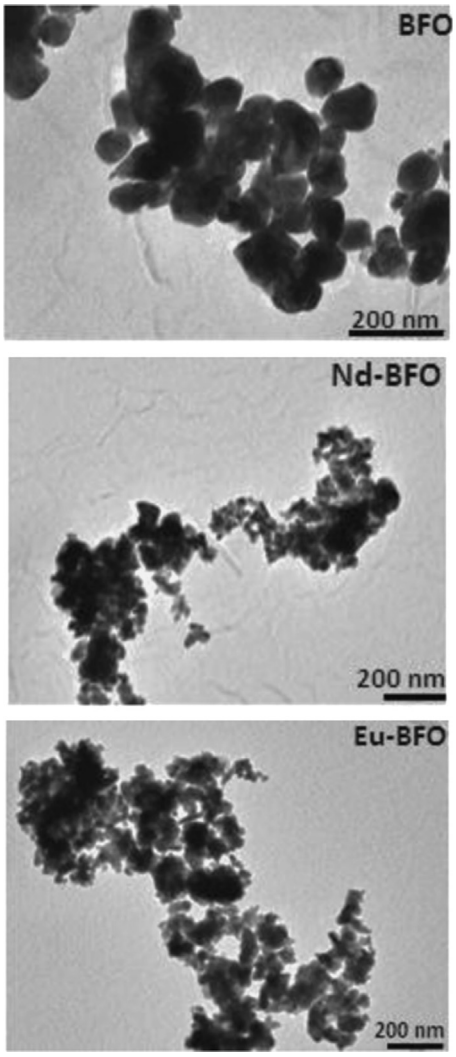

Fig. 2. TEM images of BFO, Nd-BFO and Eu-BFO.

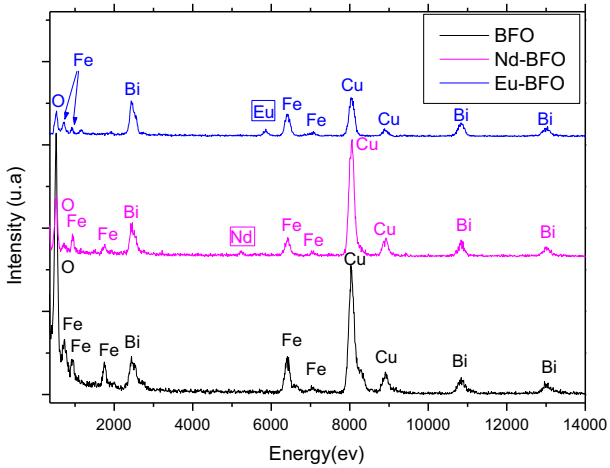

Fig. 3. EDX analysis of BFO, Nd-BFO and Eu-BFO.

The BFO and RE-BFO were analyzed by EDX analysis (Fig. 3). The Cu signal is due to the sample holder. The results confirm the stoichiometries of the samples and indicate that the RE (Nd, Eu) is smoothly incorporated into the BFO host lattice.

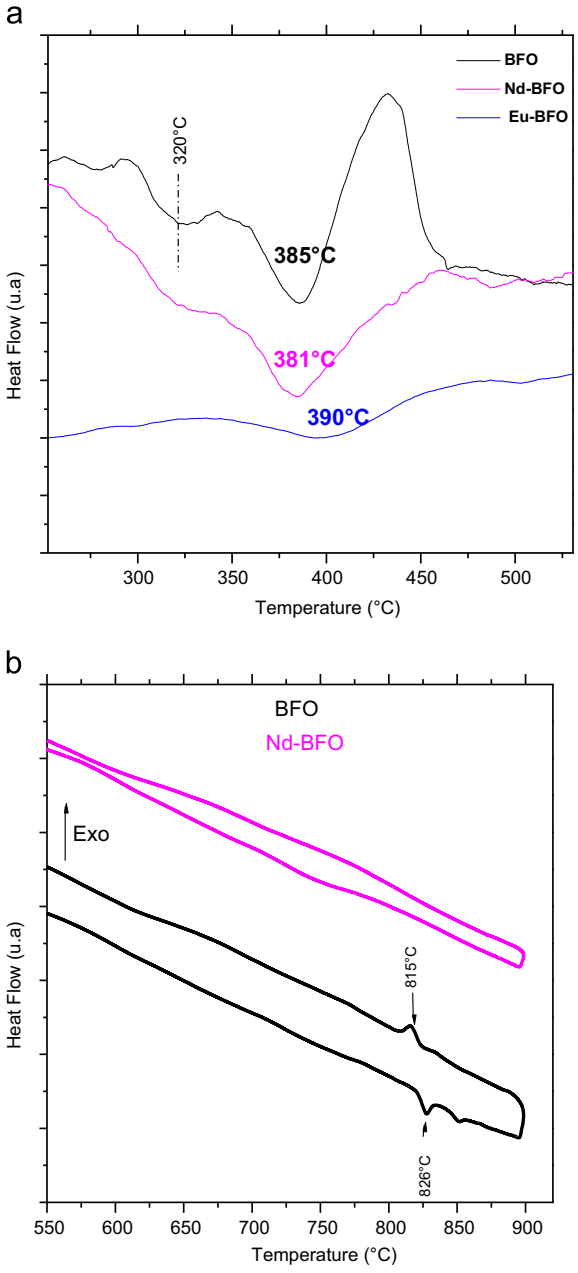

Fig. 4. The DSC curves of BFO, Nd-BFO and Eu-BFO powders in the 100–600 °C range (a) and DTA curve of BFO in the 500–900 °C range (b).

The DSC curves of BFO and RE-BFO compounds are given in Fig. 4, at 100–600 °C temperature range (Fig. 4a) and the DTA curves at 500–900 °C with heating and cooling rates of 10 °C/min under Argon atmosphere (Fig. 4b). Different thermique's anomalies are noted:

(a) A broad band observed at 380–390 °C is attributed to a magnetic phase transition (Neel temperature, T_N) [4]. It is found that the magnetic order temperature is not affected significantly by the substitution. The broadness of the peak gives evidence that the transition takes place in complex steps. The one endothermic peak at 320 °C was attributed to the antiferromagnetic to paramagnetic phase transition [5].
(b) The endothermic and exothermic peaks were observed at 826 °C during heating and 815 °C during cooling, respectively. This indicates the first order ferroelectric to paraelectric transition temperature from α-phase of R3c symmetry to an orthorhombic β-phase [4,6]. For the RE-BFO compounds, no anomalies in the base line have been observed around Curie temperature (T_C), which confirms the results obtained by XRD measurements which show the stabilization of γ-phase in these compounds.

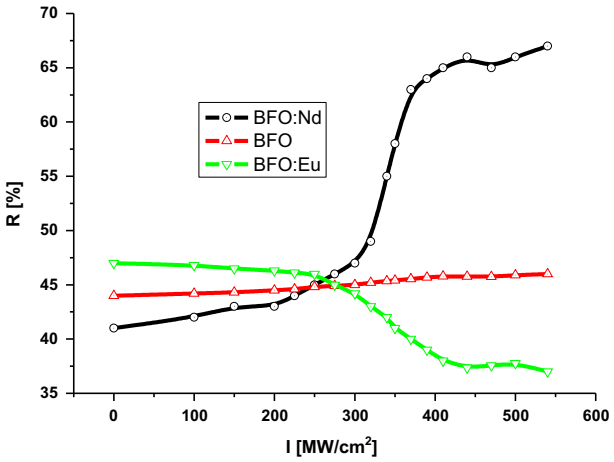

Fig. 5. Dependence of light reflection at 532 nm versus the 1064 nm pulsed laser density for pure BFO and the one doped by Nd and Eu.

Fig. 5 exhibits the dependences of light reflection at the wavelength 633 nm versus Nd:YAG laser power density. Following the presented figure, one can clearly see that the behavior is principally different for the pure BFO and the rare earth doped samples. For the pure BFO the dependence is almost constant. Depending on the type of the rare earth the dependence is quite different. For the Eu^{3+} doped the dependence decreases while for the Nd^{3+} it increases. It may be caused by different polarizabilities of the particular ions [13–15] defining the different photoinduced behaviors. Moreover, in all the cases the role of the phonon subsystem is quite different.

4. Conclusions

For the first time it was demonstrated that the doping of the $BiFeO_3$ by the rare earth demonstrates substantially different behavior versus the external laser light. For the Eu^{3+} doped the dependence decreases while for the Nd^{3+} it increases. It may be caused by different polarizabilities of the particular ions defining the different photoinduced behaviors. Moreover, in all the cases the role of the phonon subsystem is quite different.

Acknowledgments

The work was supported by CENTEM project, reg. no. CZ.1.05/2.1.00/03.0088, co-funded by the ERDF as part of the Ministry of Education, Youth and Sports OP RDI program. Computational resources were provided by MetaCentrum (LM2010005) and CERIT-SC (CZ.1.05/3.2.00/08.0144) infrastructures.

References

[1] Zhang Xingquan, Sui Yu, Wang Xianjie, Tang Jinke, Su Wenhui. J Appl Phy 2009;105::07D918.
[2] Makhdoom AR, Akhtar MJ, Rafiq MA, Hassan MM. Ceram Int 2012;38:3829–34.
[3] Zhang Xingquan, Sui Yu, Wang Xianjie, Tang Jinke, Su Wenhui. J Appl Phy 2009;105:07D918.
[4] Wei Jie, Xue Desheng. Mater Res Bull 2008;43:3368–73.

[5] Mazumder R, Sujatha Devi P, Dipten Bhattacharta, Choudhury P, Sen A. Ferromagnetism in nanoscale $BiFeO_3$. Appl Phys Lett 2007;91:062510.
[6] Wang LC, Wang Z-H, He SL, Li X, Lin PT, Sun JR, et al. Physica B 2012;407:1196–202.
[7] Kityk IV, Makowska-Janusik M, Kassiba A, Plucinski KJ. SiC nanocrystals embedded in olygoetheracrylate photopolymer matrices new promising nonlinear optical materials. Optic Mater 2000;13(N4):):449–53.
[8] Makowska-Janusik M, Kityk IV, Berdowski J, Matejec J, Kasik I, Mefleh A. Nonlinear optical phenomena in the Al_2O_3 - P_2O_5, erbium and ytterbium doped silica glasses. J. Opt A-Pure Appl Op (UK) 2000;2(N1):43–7.
[9] Kityk IV. Nonlinear optical phenomena in the large-sized nanocrystallites. J Non-Cryst Solids 2001;292(N1–3):184–201.
[10] Gruhn W, Kityk IV, Benet S. Photoinduced optical second harmonic generation in Fe-Co metallic spin glasses. Mater Lett 2002;55(N3):):158–64.
[11] Kityk IV. IR-stimulated second harmonic generation in Sb_2Te_2Se-BaF_2-$PbCl_2$ glasses. J Mod Opt 2004;51:1179–89.
[12] Majchrowski A, Kityk IV, Ebothe J. Influence of YAB:Cr^{3+} nanocrystallite sizes on two-photon absorption of YAB:Cr^{3+}. Phys Status Solidi 2004; B241:3047–55.
[13] Ebothe J, Kityk IV, Benet S, Claudet B, Plucinski KJ, Ozga K. Photoinduced effects in ZnO films deposited on MgO substrates. Opt Commun 2006;268:269–72.
[14] Kassab LRP, Hora WG, Piasecki M, Bragiel P, Kityk IV. Enhancemnt of second-order susceptibilities of Er doped germanate glasses. Opt Commun 2007;269:148–51.
[15] Ozga K, Nouneh K, Slezak A, Kityk IV. Transport and nonlinear optical study of semimagnetic phase transitions in ternary alloys $Pb_{1-x}R_xTe$ (R=Pr3+, Gd3+). J Alloys Compd 2008;448:49–52.